Cement & Concrete Composites 37 (2013) 37–46

Contents lists available at SciVerse ScienceDirect

Cement & Concrete Composites

journal homepage: www.elsevier.com/locate/cemconcomp

Sealing process induced by carbonation of localized cracks in cementitious materials

Harifidy Ranaivomanana [a], Jérôme Verdier [a,*], Alain Sellier [a], Xavier Bourbon [b]

[a] Université de Toulouse, UPS, INSA, LMDC (Laboratoire Matériaux et Durabilité des Constructions), 135 Avenue de Rangueil, F-31 077 Toulouse Cedex 04, France
[b] Andra, Parc de la Croix Blanche, 1-7 Rue Jean Monnet, F-92 298 Chatenay Malabry Cedex, France

ARTICLE INFO

Article history:
Received 22 April 2011
Received in revised form 6 November 2012
Accepted 10 December 2012
Available online 20 December 2012

Keywords:
Crack
Healing
Carbonation
Decalcification
Percolation
Leakage rate

ABSTRACT

The healing of cracks plays an important role with regard to the air- and water-tightness of concrete structures and the durability of cement based materials in general. This paper aims at further characterization and better comprehension of the healing phenomenon induced by the precipitation of calcite in localized cracks. The experimental program consisted in generating a localized crack in a cement paste or concrete specimen and healing the crack created by percolation tests with carbonated water or gas (CO_2-air mixture). For tests with liquid, results show that the healing process depends on physical parameters like crack width, pressure gradient and carbonate content in the percolating fluid. For tests with gas, the supply of the crack with Ca^{2+} ions to form calcite depends on the moisture transport mode on the crack edges, conditioned by the relative humidity of the percolating gas mixture. A simplified model of the leakage rate evolution is proposed. It provides indications concerning the effect of each test parameter on the healing process and allows the experimental results to be reproduced. Application of the model to other tests from the literature shows its limits and gives guidance for future investigations.

1. Introduction

The assessment of concrete structure lifetimes by modeling is necessary for the design of durable structures. Modeling requires a comprehension not only of the degradation phenomena but also of the healing phenomena, which improve the durability of structures. The healing process plays a very important role with regard to the sealing properties of storage or containment structures (nuclear waste repository structures in deep geologic formations, tanks, containment vessels of nuclear plants). This paper aims to characterize the phenomenon and to propose a simplified model of the leakage rate evolution.

In the presence of water, hydrated or anhydrous cement grains can react between crack edges and form crystals whose accumulation leads to the sealing of the crack. The main factors involved in the process include the continuation of the hydration process of anhydrous cement grains and/or the precipitation of calcium carbonates [1,2]. The continuation of the hydration process is significant only on a material with a large anhydrous content. This was not the case in our study materials, in which the water/cement ratio (w/c) and the curing duration ensured sufficient hydration (see Section 2). Moreover, this mode of crack healing mainly concerns the sealing of microcracks as the size of the hydration products is generally less than 10 μm. Studies on the mechanical effects of the healing process induced by the continuation of the hydration process have been published by Granger et al. [3].

This study focuses only on the healing process induced by the precipitation of calcium carbonate crystals in the crack. This crack healing mode was highlighted during tests in static conditions by keeping the fractured specimens in ambient air with a relative humidity (RH) of 100% [4]. The progression of the healing process was assessed by measuring gas output flow during percolation tests on the fractured specimen. Tests performed under dynamic conditions also allowed a healing phenomenon induced by carbonation [2,5]. The mechanisms of such a process are reported by Edvardsen [2]. Calcium carbonate, $CaCO_3$, is produced by the chemical reaction between Ca^{2+} ions from the material and CO_3^{2-} ions from the percolating water.

$$Ca^{2+} + CO_3^{2-} \rightarrow CaCO_3 \quad (1)$$

The carbonated water flows through the crack at a pH between 5.5 and 7.5. It may contain Ca^{2+} ions that are undersaturated in relation to calcium carbonate precipitation. The pH gradient between the pore solution and the percolating water leads to the dissolution of the cement matrix hydrates, providing calcium ions to the percolating water. The increase in calcium ion concentration associated with a high pH value and a low velocity of water close to the crack walls promotes the precipitation of calcite. At the beginning of the healing process, the formation of calcite crystals

* Corresponding author. Tel.: +33 5 61 55 99 19; fax: +33 5 61 55 99 49.
E-mail address: verdier@insa-toulouse.fr (J. Verdier).

0958-9465/$ - see front matter © 2012 Elsevier Ltd. All rights reserved.
http://dx.doi.org/10.1016/j.cemconcomp.2012.12.008

is controlled by the surface of the crack walls, which supply calcium ions to the crack (surface-controlled). When this calcium source becomes exhausted, the area adjacent to the crack continues to supply Ca^{2+} ions by diffusion (diffusion-controlled). In this case, the healing process becomes slower because the diffusion kinetics of calcium ions through the material and the calcite layer already formed are much slower than the precipitation kinetics. If gaseous CO_2 flows through the crack, its walls may be subject to drying. In this case, the removal of calcium ions from the pore solution to the crack edges is ensured by the convective transport of water due to the moisture gradient between the pore solution and the crack. As a consequence of the drying process, the gaseous CO_2 penetrates the area inside the crack and dissolves to form CO_3^{2-} ions. The next step is then the chemical reaction between Ca^{2+} and CO_3^{2-} ions to form calcium carbonates.

By assuming that the flow through cracks is similar to a laminar flow between parallel-sided plates, the initial output water and gas flows often referred to as Poiseuille law and deduced from Navier–Stokes equations, can be written as (2) and (3):

$$q_{0,l} = \frac{bw^3}{12\eta_l}\frac{(P_e - P_s)}{d} \tag{2}$$

$$q_{0,g} = \frac{bw^3}{24\eta_g}\frac{(P_e^2 - P_s^2)}{P_s d} \tag{3}$$

where $q_{0,l}$ (m^3/s) is the initial output water flow, $q_{0,g}$ (m^3/s) is initial output gas flow, P_e (Pa) is inlet pressure, P_s (Pa) is outlet pressure, d (m) is flow path length, b (m) is crack length, w (m) is crack width, η_l (Pa s) is dynamic viscosity of liquid, and η_g (Pa s) is the dynamic viscosity of gas, $q_{0,i}$ (i = l or g) corresponds to the initial flow value when the healing process is occurring at the same time. This initial flow value has to be corrected by a reduction factor comprising the tortuosity and the roughness of crack edges and the local irregularities of crack width. If there is no interaction between the material and the fluid flowing through the crack, the reduction factor is theoretically independent of the nature of the fluid. However, short range forces acting between water molecules and cement matrix reduce the flow rate of liquid water near the crack walls where the flow takes place. This explains why water permeability and gas permeability values are not of the same order of magnitude [6]. Therefore, two different values of the reduction factor, noted ξ_l for liquid and ξ_g for gas, have to be considered. Eqs. (2) and (3) are therefore modified as follows:

$$q_{0,l} = \xi_l \frac{bw^3}{12\eta_l}\frac{(P_e - P_s)}{d} \tag{4}$$

$$q_{0,g} = \xi_g \frac{bw^3}{24\eta_g}\frac{(P_e^2 - P_s^2)}{P_s d} \tag{5}$$

Numerous values of the ξ_l and ξ_g are proposed in the literature (see Table 1). Some authors argue that these coefficients do not have fixed values but depend on test parameters such as crack width [7–10].

Table 1
Values of the coefficients ξ_l and ξ_g proposed in the literature.

ξ_l		ξ_g	
Edvardsen [2]	0.25	Buss [13]	0.08
Ripphausen [9]	$\frac{1}{1+0.2\times10^{-3}(\frac{d}{w})^{1.5}}$	MacGregor et al. [14]	0.36
Clear [11]	0.125	Saito et al. [15]	0.249
Mivelaz [12]	0 if w 0.05 mm 0.2 if w/0.25 mm Linear interpolation between the 2 extreme values		

On the basis of her experimental results, Edvardsen [2] has proposed an empirical model of the output water flow evolution versus time (6):

$$\frac{q(t)}{q_{0,l}} = 65 w_m^{-1.05} t^{(-1.3+4w_m)} - 10^5 w_m^{5.8} \tag{6}$$

where w_m (mm) is the mean value of the crack width, $q(t)$ (l/h) is output water flow at time t, and t (h) is the time of exposure to water.

Relationship (6), based on statistical criteria, takes only the crack width into account as the physical parameter and does not restitute the initial output flow value at $t = 0$.

In accordance with the aims of this paper, a new model of leakage rate evolution, based on more physical criteria compared to Eq. (6), is proposed in the framework of the study. Of course, the development of the model also requires determination of the appropriate value of the reduction factor ξ_l in order to obtain a correct prediction of the initial outlet flow of water. For this purpose, percolation tests were performed on fractured specimens with carbonated water or gas (CO_2-air mixture). The experimental program is described in detail in the next section.

2. Experimental program

2.1. Materials

Tests were carried out on ring-shaped concrete and cement paste samples (noted C and CP respectively) made with CEMI cement (CEMI 52.5 PM ES-Val Azergues, Lafarge), the chemical composition of which is given in Table 2.

The cement paste was made with a w/c ratio of 0.5. The concrete was a high-performance concrete (HPC). The samples were stored in endogenous curing conditions in a temperature controlled room at 20 °C for over 2 months, in order to reach a pronounced degree of hydration. On materials of the same type, Baroghel Bouny [16] measured a degree of hydration close to 1 after three months of storage in endogenous cure conditions. This implies that the healing process induced by the continuation of the hydration process was very limited in our case. The formulation of the materials and their physical characteristics are recorded in Table 3.

The relative permeabilities to liquid of the study materials are important with regard to the healing process, especially for gaseous CO_2 percolation. In this case, the removal of calcium ions from the pore solution to the crack edges is ensured by the convective transport of water due to the moisture gradient between the pore solution and the crack. This convective flow is given by the product of the intrinsic permeability and the relative permeabilities to liquid that we calculated by considering the pore network model developed by Ranaivomanana et al. [17].

The samples were saturated under vacuum before the percolation tests. This saturation was necessary to avoid moisture gradients within the material, which could have affected the healing process as, whatever the nature of the percolating fluid, healing is possible only if the internal humidity value of the material remains very high. This is not the case after the storage in endogenous cure conditions leading to a degree of saturation corresponding to a RH of 90% for concrete (C) and of 95% for cement paste (CP).

2.2. Generation of a crack and width measurement

A crack was generated in the ring-shaped sample by using the "expansive-core" system developed by Gagné et al. [18].

The "expansive-core" system is composed of four main components: a steel cone, a clamping base, 6 steel petals and a PVC ring

Table 2
Chemical composition of the cement used.

	SiO_2	Al_2O_3	Fe_2O_3	CaO	MgO	SO_2	Na_2O	K_2O	Loss on ignition
% By mass	20.90	3.20	4.60	65.10	0.60	2.76–3.00	0.10	0.60	1.25

Table 3
Mix design and characteristics of test mixtures.

	(C)	(CP)
Cement (kg/m^3)	400.0	1218.0
Limestone sand (0/4 mm) (kg/m^3)	858.0	–
Limestone gravel 4/12.5 mm (kg/m^3)	945.0	–
Super plasticizer (kg/m^3)	10.0	–
Total water (kg/m^3)	178.0	609.0
Porosity (%)	12.3	45
Dry density (kg/m^3)	2349.0	1451.0

(Fig. 1). The cone is placed at rest on the petals inside the PVC ring. By using the clamping base and the nut, the cone is gradually brought down in order to increase the spacing on the petals. This action increases the diameter of the PVC ring, which transmits its deformation to the sample. The sample is then subjected to a tensile stress field which generates the cracking. We ensured that a single crack was obtained by inserting an incomplete reinforcement (rod diameter = 6 mm) in the sample. The crack appeared in the area of the sample corresponding to the missing part of the reinforcement, where the strains were supported by the material only. This area had a smaller height (30 mm) than the rest of the sample (50 mm) because it was topped by a sleeve in which a transducer was inserted for crack width measurement (Fig. 1). In order to impose a radial path on the crack, the sleeve edges, which are singular zones, were oriented along two radii of the sample. One of them was fitted with a small slot and the other with a rounded corner in order to locate the crack in the less resistant zone. These cracking tests were carried out in the percolation cell, which was topped with a metal lid. This prevented direct measurement of the crack width by videomicroscope (Fig. 2) and is the reason why we developed the transducer mentioned previously. It consisted of two flexible stainless metal rods to which strain gauges were bonded. The crack width corresponded to the rod displacements correlated to with the strain values indicated by the gauges. The accuracy of the transducer was +/−10 μm.

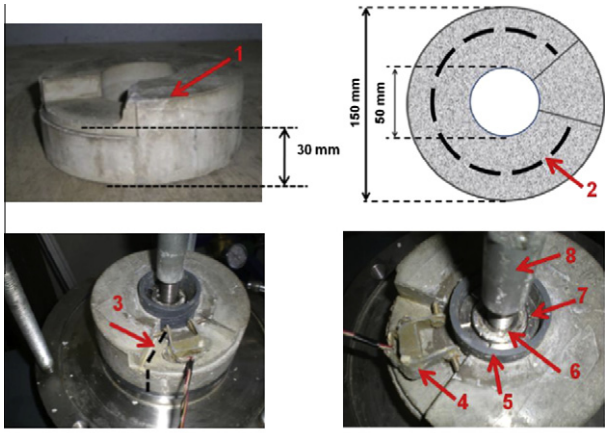

Fig. 1. Cracking tests on ring-shaped specimen.

2.3. Description of the experimental device for percolation tests

For the percolation tests, an experimental device was developed. It included two systems that could be used separately: one for liquid and the other for gas. The percolating fluid was carbonated water or gas (CO_2 air-mixture), prepared in a sealed Plexiglas cell (Fig. 2) with a CO_2 sensor connected to a solenoid valve, itself connected to a CO_2 source. The device kept the CO_2 partial pressure value constant at 5% of atmospheric pressure. If the percolating fluid was gas, the relative humidity of the gas mixture was the same as in the external environment (60%). As mentioned previously, this is a limiting factor with regard to the healing process. The carbonated water was prepared by pouring 30 l of deionized water into the Plexiglas cell. It was then transported via a hydraulic pump to a membrane cell that controlled the differential pressure between the inlet and outlet of the crack. In the percolation cell, the seal at the external surface of the ring-shaped sample was ensured with a silicone membrane subjected to confining pressure with a minimum value equal to 1.5 times the differential pressure, which did not exceed 1 bar in the framework of this study. The seal at the internal surface of the sample was ensured by the contact between the PVC ring and the sample itself. If the output flow value remained zero until the generation of the crack, the seal was guaranteed to be effective. The output water flow was measured by weighing using a balance connected to a computer to acquire the data. The outlet gas flow was measured with a flowmeter. An overview of the device is provided in Fig. 2.

As mentioned previously, tests of the same type were carried out by Edvardsen [2]. She used water in equilibrium with atmospheric CO_2 content as the percolating fluid. Three crack widths (100, 200 and 300 μm) were tested at different pressure gradients between 0.625 and 5 bar/m (height of flow equal to 40 cm). The results obtained by Edvardsen showed a reduction of the leakage rate over time as a result of the crack healing phenomena. They also highlighted the fact that a crack could not seal if its width was greater than a "threshold" value, which depended on the pressure gradient considered. This "threshold" crack width was between 200 and 300 μm for the pressure gradients 0.625 and 1.25 bar/m. For pressure gradients greater than 2.5 bar/m, the sealing of a 200 μm-wide crack no longer seemed to be possible. By analyzing the percolate, Edvardsen still detected the presence of HCO_3^- ions but especially CO_3^{2-} ions, revealing that the CO_2 partial pressure was not a limiting factor regarding the healing process. Compared to the results obtained by Edvardsen [2], we could not impose a pressure gradient smaller than 2.5 bar/m for our percolation tests with carbonated water, due to the small height of flow (30 mm). Thus, the "threshold" crack width value corresponding to our experimental conditions should not exceed 200 μm. The percolation tests with carbonated water were performed on 2 cement pastes (CP) and 3 concretes (C). Due to the difficulty in controlling the initial crack width, we could not impose a definite value for it. However, the range of crack opening involved in our tests was well known, varying from 15 to 240 μm. The test parameter values ($\Delta p, b, d, w$) and the initial output flow value (q_{ini}) for each test are reported in Table 4.

The evolution of the output flow in the case of liquid was recorded until it stabilized a minimum duration of 24 h until it had been stable for at least 24 h.

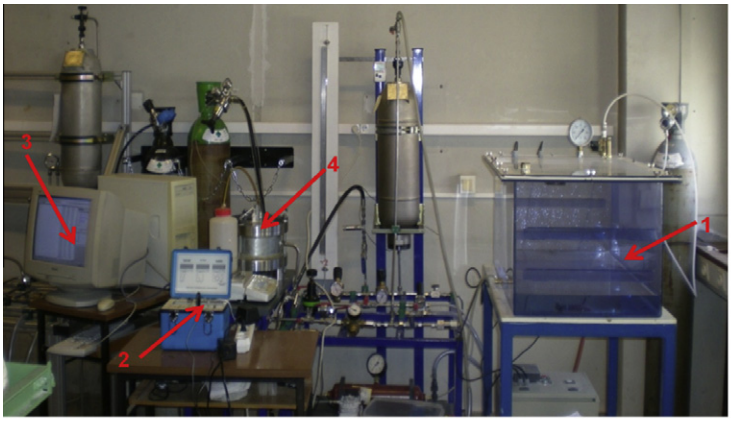

1: Plexiglass cell for percolating fluid preparation
2: Strain gauge bridge connected with the transducer inserted in the sample
3: Water flow acquisitions
4: Percolation cell

Fig. 2. Experimental device for percolation tests.

Table 4
Values of the experimental parameters and initial water output flow for each specimen tested during water percolation tests.

	Sample reference	Δp (bars)	b (m)	d (m)	w_0 (μm)	q_{ini} (g/min)
(CP)	CP-1	1.0	0.05	0.03	15	0.78
	CP-2	0.1			135	50.32
(C)	C1	0.1			147	65
	C2	0.2			111	56
	C3	0.1			240	283

Characterization tests (SEM observations coupled with EDS, video microscope observations and XRD analysis) were subsequently carried out to highlight the phenomena involved in the healing process. After percolation tests with water, two fragments associated respectively with each fracture surface are removed by sawing from the specimens tested (cement pastes and concretes). The first fragment is used for SEM observations. It is first sliced perpendicularly to the fracture surface as shown in Fig. 3. After that, the lower and upper surfaces of each slice obtained are coated with a thin layer of conducting metal to avoid the deflection of the trajectories of the electrons which results in a grossly distorted image. For this purpose, gold is chosen instead of carbon since the healing process is closely related to carbonation phenomenon. During SEM

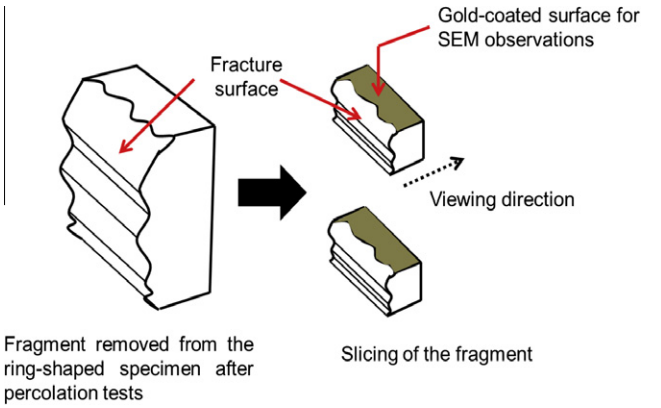

Fig. 3. Preparation of the samples for SEM observations.

Table 5
Values of the experimental parameters for each specimen tested during gas percolation tests.

	Sample reference	ΔP (bars)	b (m)	d (m)	w_0 (μm)	q_{ini} (l/h)
(C)	C4	0.04	0.05	0.03	190	0.252
	C5	0.01			400	0.270
(CP)	CP-3				600	0.300

observations, two levels of magnification were considered: 200× and 500× respectively. The second fragment is used for observing the fracture surface with video microscope. No particular treatment of the sample is required in this case.

Three percolation tests with gas were performed in addition to the preliminary tests required for the commissioning of the experimental device shown in Fig. 2. The first two were conducted on concrete (C) (samples C4 and C5) and the third on cement paste (CP) (sample CP-3). The initial crack widths were 190, 400 and 600 μm. The differential pressure values were 0.04 bar for the first test and 0.01 bar for the two others. They were weaker for these tests with gas than for the tests with water, due to a dynamic viscosity of the gas mixture ($\eta_g \sim 18.5 \times 10^{-6}$ Pa s) lower than that of water ($\eta_l \sim 10^{-3}$ Pa s). Of course, the confining pressure values were lower and this affected the control of the crack width, resulting in the creation of wider cracks. The test parameter values and the initial output gas flow for each sample tested are presented in Table 5.

3. Experimental results and analysis

3.1. Percolation tests with gas

The initial output flows were quite similar for the three tests despite the difference between the three crack width values. This result may be explained by the heterogeneity of the crack widths between the internal and the external surfaces of the samples. This was probably due to the weakness of the confining pressures. The crack width values provided by the transducer may be questionable in this case because their measurement was punctual. It would have been wiser to use the output flow values q_{ini} to determine the crack width values using Eq. (5) validated in numerous research works. For this purpose, an estimation of the appropriate value of the coefficient ξ_g would have been necessary. However,

the determination of this coefficient was not treated in the framework of this study due to the limited number of tests.

After 2 h of gas pressure exposure, no evolution of the output flow was observed on the three samples. This can be explained by the following:

- Wider open cracks promoting the flows and limiting the interactions between the fluid and the cement matrix. Thus, a small amount of CO_2 was fixed on crack walls.
- Due to the drying of the crack edges, ensured preferentially by water vapor diffusion, which prevented the supply of the crack with Ca^{2+} ions, the healing potential was limited in the case of percolation tests with gas. Moreover, during the drying of the crack edges, CO_2 could penetrate into the material. The carbonation reactions then led to the sealing of the capillary porosity near the crack walls as pointed out by Bary and Sellier [19]. This would compromise the removal of calcium ions, resulting in a lower healing potential.

3.2. Percolation tests with carbonated water

3.2.1. Influence of test parameters

For each sample tested, the evolutions of the output flow of water versus time are shown in Figs. 4 and 5.

The output flows of water measured during tests were only attributable to the crack because the rest of the specimen was considered to be impermeable. This hypothesis was, of course, validated for tests with gas, but also for tests with water because of the low values of the differential pressures leading to a very long time to reach the steady state regime in the non-fractured part of the samples. Evolutions of the output flow highlight physico-chemical changes inside the crack due to the movement of grains and/or local chemical imbalances, like the precipitation of calcium carbonates. Referring to the results obtained by Edvardsen [2] for a crack width of 100 μm and a pressure gradient of 2.5 bar/m, the output flow decreased by 50% of its initial value after 50 h of exposure to carbonated water. However, in the case of cement paste CP-2 with a crack width equal to 135 μm and subjected to a pressure gradient of the same order of magnitude, the attenuation of the initial output flow was over 99% for the same duration. It can be deduced that not only the carbonate content of the percolating solution but also the amount of available calcium help to accelerate the healing process in its initial phase. The greatest attenuation of the output flow was observed on the concrete C-1 and on the cement paste CP-2, for which differential pressures were the lowest (0.1 bar). Video-microscope observations (magnification up to 175×) of concrete C-1 at the end of the test highlighted the sealing of the crack (Fig. 6).

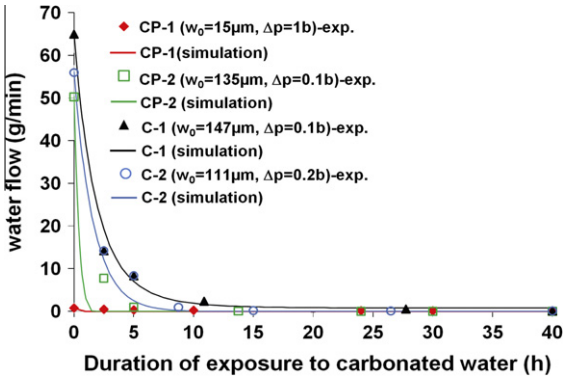

Fig. 4. Evolution of the output water flow on cement pastes CP1 and CP2, and on concretes C1 and C2: experimental results (symbols) and simulation results (solid line).

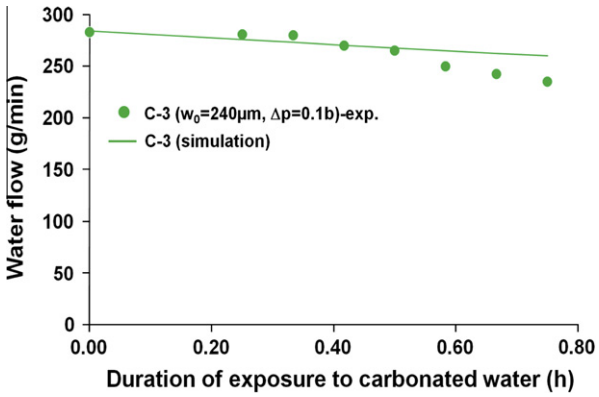

Fig. 5. Evolution of the output water flow on concrete C3: experimental results (symbols) and simulated results (solid line).

These results reveal that the pressure gradient can be a limiting factor with regard to the sealing of a crack. This is corroborated by the results obtained on the cement paste CP-1 subjected to a differential pressure of 1 bar, for which a residual leakage rate could be measured after more than 100 h of percolation despite the small crack width value (15 μm). Similar results were obtained on concrete C-2 subjected to a differential pressure of 0.2 bar despite the fact that the crack width value was lower than those of specimens C-1 and CP-2. Concerning the concrete C-3, the leakage rate could not be recorded beyond one hour of percolation because of a more open crack (240 μm) resulting in a high output water flow and a rapid emptying of the membrane cell. Nevertheless, low attenuation of the output flow could be observed.

3.2.2. Highlighting of the phenomena involved in the healing process

As mentioned previously, characterization tests (SEM observations coupled with EDS and XRD analysis) were carried out in order to highlight the phenomena involved in the healing process. These phenomena are decalcification and carbonation. The first SEM observations were performed on one of the crack surfaces belonging to the cement paste CP-1. The corresponding pictures showed a field of calcium carbonate covering the entire surface of the crack (Fig. 7a). These calcium carbonate crystals were identified by XRD analysis to be calcite (Fig. 7b). The metastable varieties of calcium carbonates, vaterite and aragonite, were not detected because they are formed at low RH [20]. In the framework of this

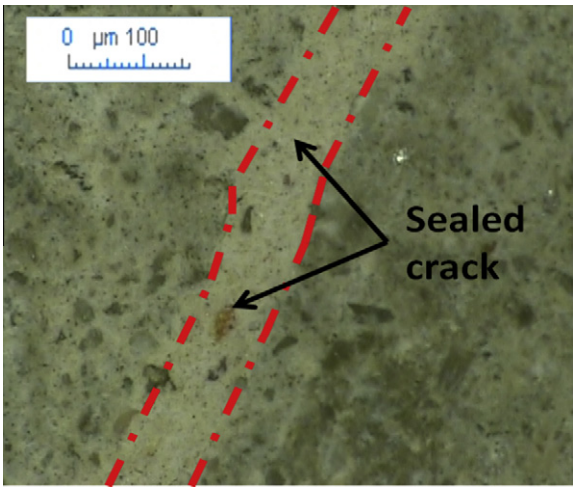

Fig. 6. Picture of the sealed crack in concrete C-1 (175x).

study, the healing process was thus exclusively associated with the carbonation and not with a possible continuation of the hydration process because the acidic pH value of the carbonated water prevented the formation of portlandite or C–S–H on the crack surface.

Another sequence of observations was conducted on cement paste CP-2 and on concrete C1 in order to quantify the thickness of the calcite layer on the crack surface. However, this quantification was very difficult, not to say impossible, to perform because the fracture surface was not flat but had an irregular slope (see Fig. 3). This prevented correct estimation of calcium rates. In order to characterize the decalcification process occurring in the cementitious matrix behind the crack surface, the SEM observations were coupled with EDS analysis (Fig. 8). A gradual increase in CaO content immediately adjacent to the crack surface can be observed in Fig. 8. The area concerned is then subjected to a decalcification process, extending to a depth of about 30–60 μm. The horizontal line on Fig. 8 corresponds to the CaO content of the sound cement matrix, estimated to be 60% using the approach proposed by Adenot [21]. It is based on the determination of the amount of hydrates formed, using the chemical composition of the cement, the formulation of the material and the degree of hydration as input.

3.3. Leakage rate modeling

3.3.1. Initial output flow of water

The prediction of the initial output flow of water involved the determination of the adequate value of the reduction factor ξ_l which appears in Eq. (4). The initial output flow values (noted q_0), obtained using Eq. (4) for the different values of ξ_l recorded in Table 1, are presented in Table 6 with respect to the accuracy of the transducer (+/−10 μm).

From the three values of ξ_l used to evaluate the initial leakage rate, the one proposed by Edvardsen [2] ($\xi_l = 0.25$) provides initial output flow values comparable to those measured experimentally (q_{ini}). We therefore decided to adopt this value for our study.

3.3.2. Evolution of the leakage rate over time

As mentioned previously, the empirical model proposed by Edvardsen [2] to predict the evolution of the leakage rate over time (Eq. (6)) includes only the initial crack width value as a test parameter and does not allow the initial output flow at $t = 0$ to be restituted.

A more appropriate model of the leakage rate evolution based on physical criteria was therefore developed. For this purpose, we used Eq. (4) by hypothesizing that the leakage rate evolution was due only to the evolution of the crack width. We assumed that tortuosity and roughness effects were constant in order to limit the number of calibration parameters.

Then Eq. (4) takes the form:

$$q(t) = \xi_l \frac{b[w_0 - 2e(t)]^3}{12\eta_l} \frac{\Delta p}{d} \tag{7}$$

where t (s) is the duration of exposure to carbonated water, $q(t)$ (m^3/s) is output water flow at time t, w_0 (m) is initial crack width, $e(t)$ (m) is thickness of the calcite layer formed at time t, and p (Pa) is the water pressure differential between inlet and outlet of the crack.

We propose to describe the evolution of the thickness of calcite formed by the following exponential law:

$$e(t) = e_{max}\left(1 - \exp\left(-\frac{t}{\tau}\right)\right) \tag{8}$$

τ (s) represents the characteristic time with regard to the healing process. The lower the value of τ, the faster the crack healing.

e_{max} (m) denotes the maximum thickness of calcite which can potentially be formed. It depends on the solid calcium content of the material, noted [Cas] (mol/m^3), and the equivalent depth, e_{decal} (m), subjected to decalcification. Note that the source of calcium ions may be in a different zone of the sample depending on its geometry. It is possible that the area behind the crack surface is not the only calcium ion source because calcium can also come from the upstream side of the sample. Finally, e_{max} depends on the molar volume of calcite ($V_{calcite}$), which is 36.9×10^{-6} m^3/mol, and the porosity of the calcite layer formed. The solid calcium concentration [Cas] is calculated using the approach proposed by Adenot [21]. For cement paste (CP), we have 11605 mol/m^3 and, for concrete (C), 3776 mol/m^3. A simplified description of the healing process is proposed in Fig. 9.

The maximum thickness of calcite layer e_{max} which can potentially be formed is then given by the following equation:

$$e_{max} = V_{calcite} \times [Ca_s] \times e_{decal} \tag{9}$$

The equivalent decalcified depth e_{decal} is assumed to be a calibration parameter of the model.

We will now propose an expression for the characteristic time τ. For this purpose, we first define a characteristic time necessary for the calcite to be deposited on a crack wall (noted $t_{calcite}$) and another characteristic time, in which the carbonated water to flows through the crack (noted $t_{filtration}$). If $t_{filtration}$ is small compared to $t_{calcite}$, the calcite cannot be formed and the calcium ions are removed with the water. The crack sealing is then very slow or impossible. Conversely, if $t_{filtration}$ is high compared to $t_{calcite}$, calcite

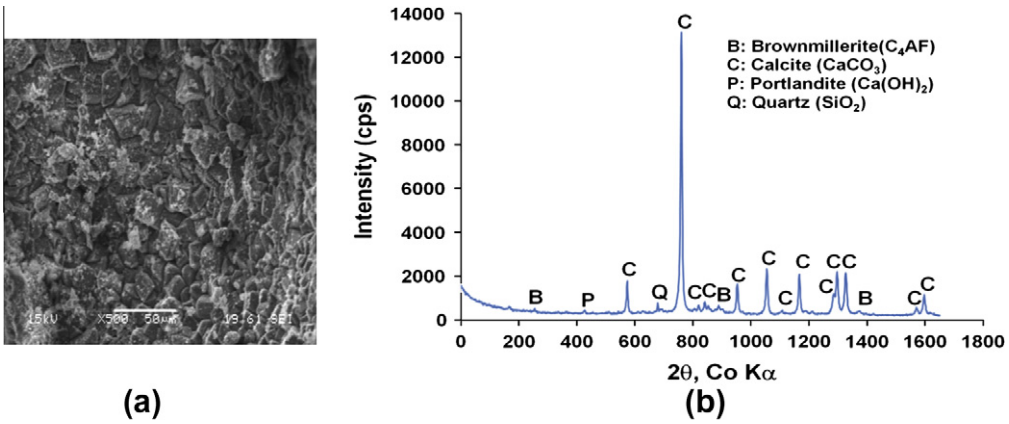

Fig. 7. Calcium carbonate field covering the crack edge (a) – identified as calcite by XRD (b).

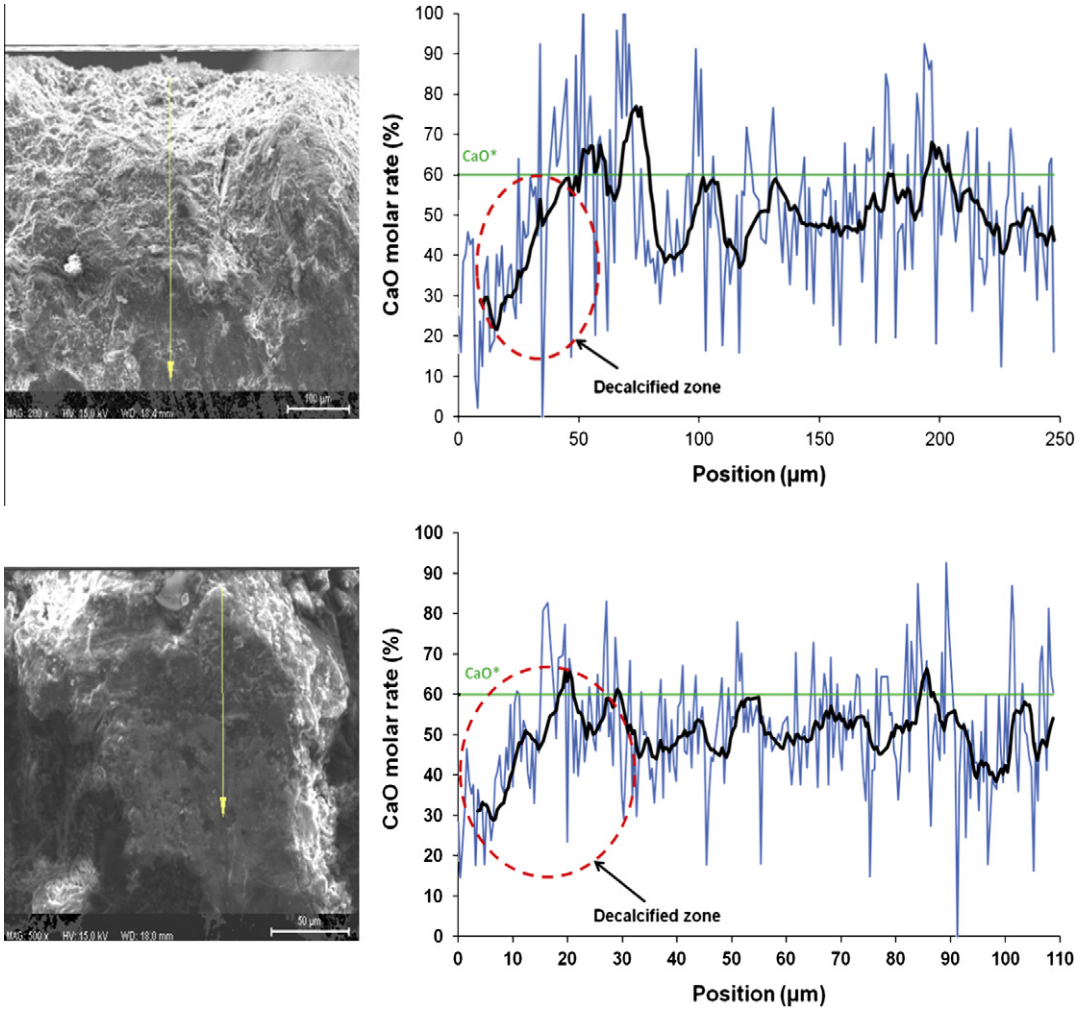

Fig. 8. Existence of a decalcified zone in the zone surrounding the crack, characterized by SEM + EDS, profiles corresponding to the line on the left figure. The line starts from the edge of the crack and penetrates into the matrix perpendicularly to the crack.

Table 6
Validation of the prediction of the initial flow for different values of ξ_l proposed in the literature.

	q_{ini} (g/min)	q_0 (g/min) Edvardsen [2] ($\xi_l = 0.25$)	q_0 (g/min) Ripphausen [9] ($\xi_l = \xi_l(w/d)$)	q_0 (g/min) Clear [11] ($\xi_l = 0.125$)	q_0 (g/min) Mivelaz [12] ($\xi_l = 10^{-3}(w - 50)$) w (μm)
CP1	0.8	0–3.2	0–1.4	0.01–1.6	0
CP2	50	40–51	93–159	20–32	12.8–16.3
C1	65	53–65	130–211	27–40	206–25.2
C2	56	42–73	85–166	21–37	10.25–17.8
C3	283	250–284	672–780	111–127	190–215.8

remains inside the crack and the healing process occurs rapidly. As a first approximation, we assume that the characteristic time τ is proportional to $t_{calcite}$ and inversely proportional to $t_{filtration}$.

$$\tau = k \times \frac{t_{calcite}}{t_{filtration}} \tag{10}$$

k (s) is the coefficient of proportionality. It is a fitting parameter which will be combined with another one below.

The time $t_{filtration}$ necessary for carbonated water to flow through the crack depends on the crack length (d) and on the fluid velocity in the crack

$$t_{filtration} = \frac{d}{v_{filtration}} \tag{11}$$

$v_{filtration}$ is obtained from Eq. (4). By combining Eqs. (4) and (11), we have:

$$t_{filtration} = \frac{12\eta_l d^2}{\xi_l w^2 \Delta p} \tag{12}$$

In Eq. (12), w evolves with time due to the crack healing. If we are interested in the initiation of the healing process, we can assimilate the crack width value w to its initial value w_0. The relationship obtained is then realistic at the beginning of the healing process.

The characteristic time $t_{calcite}$ is assumed to be inversely proportional to the rate of formation of the calcite. By adopting first-order kinetics with regard to the CO_2 partial pressure noted as P_{CO_2} (Pa) and to the calcium ion concentration [Ca] (mol/m^3) of the pore solution as proposed by various authors [19,22], we obtain relationship (13). This is a simplified approach because the calcium ion concentration [Ca] in the area adjacent to the crack is not equal to the value corresponding to the sound matrix but decreases progressively, resulting in a gradient as shown on Fig. 9. This gradient will decrease with time and the diffusion of calcium ions

from the area adjacent to the crack will also depend on the rate of saturation of the material. As the supply of the crack with Ca^{2+} ions is conditioned by the relative permeability to liquid, this

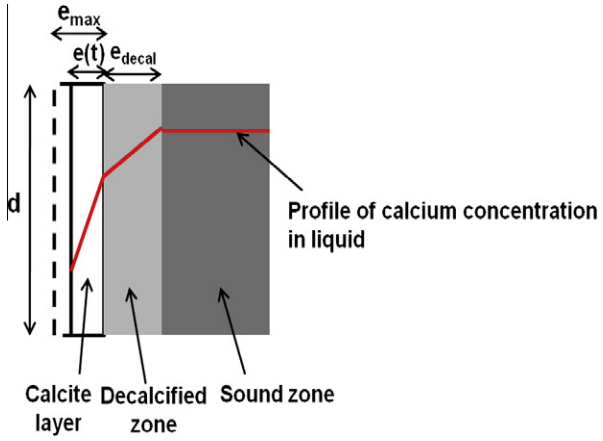

Fig. 9. Illustration of the crack healing process.

parameter can also be considered in the definition of characteristic time. Its value is, of course, equal to 1 for percolation tests with water, but may drop significantly for tests with gas, thus explaining the difficulty of crack healing in non-saturated conditions. A value of [Ca] equal to 22 mol/m^3 is adopted, corresponding to the theoretical equilibrium of portlandite with low alkaline water at 20 °C [19].

$$t_{calcite} = \frac{\kappa}{p_{CO_2} \times k_{rl} \times [Ca]} \tag{13}$$

κ is a proportionality coefficient (m^3 Pa^{-1} s^{-1}).

By combining Eqs. 10, 12, 13, we obtain:

$$\tau = k \frac{\xi_l \times \kappa \times w^2 \times \Delta p}{12\eta_l \times p_{CO_2} \times k_{rl} \times [Ca] \times d^2} \tag{14}$$

Grouping all constant terms into a single term, denoted A, gives:

$$\tau = A \frac{w^2 \times \Delta p}{p_{CO_2} \times k_{rl} \times [Ca] \times d^2} \tag{15}$$

The present model, which concerns the healing process initiation, requires two calibration parameters: A (mol s m^{-3}) and e_{decal} (m). Although relationship (15) is based on assumptions limiting its application to the beginning of the healing process, it allows the effect of each physical parameter on the process to be understood. We can observe that the characteristic time τ is proportional to the square of the crack width and to the differential pressure, but is inversely proportional to the CO_2 partial pressure, to the calcium ion concentration of the pore solution and to the square of the flow height. An increase in the relative permeability helps to reduce the value of the characteristic time τ. The reliability of relationship (15) depends on its ability to reproduce various experimental results with a single set of parameters, which were obtained by minimizing the quadratic error between experimental and simulation results: $A = 7.33 \times 10^9$ mol s m^{-3} and $e_{decal} = 4.07 - \times 10^{-4}$ m. This parameter set is unique for all tests performed in the framework of the present study. Note that the equivalent decalcified thickness e_{decal} is greater than that measured by SEM observations (~50 μm). This result is to be expected considering the explanations provided previously (calcium ion source may also be upstream of the crack, cf. Fig. 1). Moreover, the calcite layer thickness calculated by the model includes neither the tortuosity of the crack walls nor the crack width irregularities. These effects may cause local sealing that prevents the flows and limits the decalcification process in the area adjacent to the crack. The model also neglects the porosity of the calcite layer formed, which necessarily reduces the value of e_{decal}. These are the reasons why we have chosen to define the equivalent decalcified thickness e_{decal} as a calibration parameter. Despite this point, which deserves further study, the model correctly reproduces the output flow evolution during the initiation of the healing process (Figs. 4 and 5). The model results tend towards a total sealing of the crack. In reality, a low residual output flow may be observed. This is not surprising with regard to the simplifying assumptions discussed above, on which the model is based. It is important to note that the calibration of the model was performed by using our experimental results for crack width values ranging from 15 to 150 μm and differential pressure values between 0.1 and 1 bar.

We then sought to determine the values of calibration parameters corresponding to other experimental results from the studies by Schiessl and Reuter [23] (reported by Edvardsen [2]) and Reinhardt and Jooss [5]. This approach aimed to test the sensitivity of the calibration parameters corresponding to other test parameter values. These test parameter values and the experimental and theoretical values of the initial output flow are reported in Table 7.

The theoretical values of initial output flow q_0 calculated from Eq. (4) are for crack width values different from the experimental values q_{ini}. This is due to uncertainties on the crack width values. The crack width values reported in Table 7 are values that are covered but are not averaged values. To overcome these uncertainties, we prefer to use crack width values corresponding to the experimental output flow values (noted w'_0), by using Eq. (4) (see Table 8).

The percolation tests performed by Reinhardt and Jooss [5] were conducted on CEMII- based concretes with fly ash and silica fume additions. By using the approach proposed by [17] in order to take account of the pozzolanic reactions, the solid calcium content [Cas] of these materials is estimated to be equal to 2280 mol/m^3. However, for concretes tested by Schliessl and Reuter [23], we assume a solid calcium content [Cas] equal to that calculated for our materials (3778 mol/m^3) because the exact formulations of these concretes were not supplied by the author but, from their description, it can reasonably be assumed that the cement content and type were close to our material. Finally, the percolating fluid is assumed to be in equilibrium with the atmospheric CO_2 partial pressure (~0.3% of atmospheric pressure). The calibration parameter values corresponding to the previous test parameter values are presented in Table 9. The theoretical and experimental evolutions of the output water flow are shown in Figs. 10 and 11.

The value of the parameter A obtained corresponding to the results obtained by Reinhardt and Jooss [5] is of the same order of magnitude as that corresponding to our own results. This seems

Table 7
Values of the experimental parameters corresponding to percolation tests performed by Schliessl and Reuter [23] and Reinhardt and Jooss [5].

		Δp (bars)	b (m)	d (m)	w_0 (μm)	q_{ini} (g/min)	q_0 (g/min)
Schiessl and Reuter [23]	Sample 1	0.25	0.2	0.4	100	40.73	15.63
	Sample 2				200	100.00	125.02
Reinhardt and Jooss [5]	Sample 1	0.5	0.15	0.05	50	25.00	23.44
	Sample 2				100	55.00	187.50
	Sample 3				150	275.00	421.88

Table 8
Crack width values corresponding to the initial output flow measured by Schliessl and Reuter [23] and Reinhardt and Jooss [5] respectively.

		w_0 (μm)	w'_0 (μm)
Schiessl and Reuter [23]	Sample1	100	135
	Sample 2	200	190
Reinhardt and Jooss [5]	Sample 1	50	52
	Sample 2	100	70
	Sample 3	150	115

Table 9
Values of the calibration parameters for percolation tests performed by Schliessl and Reuter [23] and Reinhardt and Jooss [5].

	A (10^9 mol s m^{-3})	e_{decal} (μm)
Schiessl and Reuter [23]	234	424
Reinhardt and Jooss [5]	8.2	279

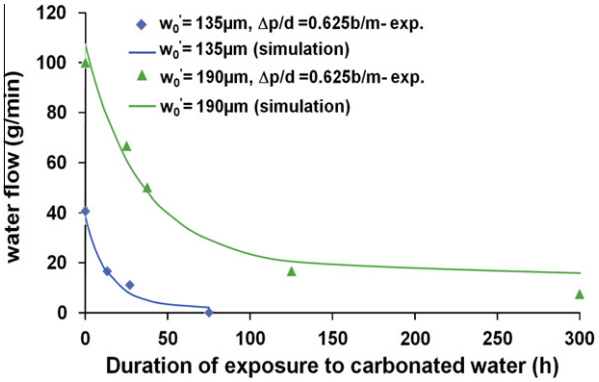

Fig. 10. Evolution of the output water flow during percolation tests performed by Schliessl and Reuter [23]: experimental results (symbols) and simulated results (solid line).

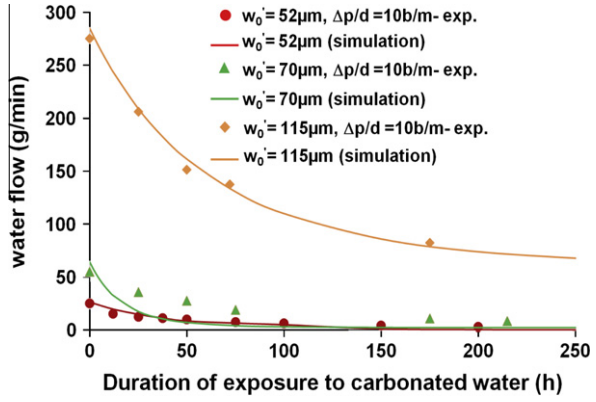

Fig. 11. Evolution of the output water flow during percolation tests performed by Reinhardt and Jooss [5]: experimental results (symbols) and simulated results (solid line).

reasonable because the flow heights are relatively close. For Schiessl and Reuter [23], who performed their tests on samples of greater height (400 mm), the value of the parameter A is larger. The dependence of parameter A on the height of the sample indicates that the consideration of this parameter in the gradient term and in the characteristic time $t_{filtration}$ would be insufficient. It would be desirable to incorporate probabilistic information concerning the constrictivity of the crack as, the higher the sample, the greater the probability of sealing by constrictivity. This aspect of transport in a fractured medium is certainly a perspective for our study. According to the equivalent decalcified thickness e_{decal}, the calcium ions which precipitate into calcite inside the crack do not come only from the area adjacent to the crack but probably also from the other zones of the tested samples and even from the percolating solution itself. This fact has been observed previously and it is not surprising to find it again here.

4. Conclusions

In order to characterize the crack healing process induced by carbonation, percolation tests were performed on fractured specimens. For this purpose, an experimental device was developed. It includes the "expansive core" system for creating a crack in ring-shaped specimen, a transducer for measuring the crack width and a percolation setup with two systems which can be used separately for liquid (carbonated water) or for gas (gaseous CO_2 + humid air).

In the case of tests with gas, it has been highlighted that the crack healing process depends strongly on the relative humidity of the gas mixture. Indeed, relative humidity defines the transport mode of moisture during the drying of the crack edges and hence the supply of calcium ions to the crack to form calcite.

In the case of tests with carbonated water, the results obtained revealed that the pressure gradient is a limiting factor with regard to the sealing of the crack. This seems to confirm the existence of a "threshold" crack width value associated with the pressure gradient value, as observed in a previous study [2]. If the initial crack width value is greater than this "threshold" value, the crack cannot seal. The carbonate content of the percolating fluid contributes to the acceleration of the healing process only in its initial phase when Ca^{2+} ions are still available on the crack surfaces. The precipitation of calcite on the crack surfaces was verified, as was the decalcification process which occurred in the area adjacent to the crack. In the framework of the present study, we have validated some of the approaches proposed in the literature which aim to predict the initial leakage rate.

We have subsequently proposed a simplified model of the evolution of the leakage rate (tests with carbonated water) versus time. The originality of the model developed lies in its simplicity (2 calibration parameters) and in the consideration of the physical parameters (crack width, pressure gradient, carbonate content, solid calcium content of the material, calcium ion concentration of the pore solution) and the phenomena involved in the healing process (carbonation and decalcification). The simulation results show that the decalcified area behind the crack surface is not the only zone responsible for the crack healing. It is also necessary to take an external source of calcium into account. Moreover, variations of the tortuosity and the constrictivity effects and the porosity of the calcite layer formed inside the crack have to be considered in order to establish a realistic model which is less dependent on experimental conditions.

Acknowledgment

We wish to express our thanks to Andra (French National Agency for Radioactive Waste Management) for its scientific and financial support for the project that led to this study.

References

[1] Hearn N. Self sealing, autogenous healing and continued hydration, what is the difference. Mater Struct 1998;31(8):563–7.
[2] Edvardsen C. Water permeability and autogenous healing of cracks in concrete. ACI Mater J 1999;96(4):448–55.
[3] Granger S, Loukili A, Pijaudier-Cabot G, Chanvillard G. Experimental characterization of the self healing of cracks in an ultra high performance

cementitious material: mechanical tests and acoustic emission analysis. Cem Concr Res 2007;37(4):519–27.
[4] Ismail M, Gagné R, François R, Toumi A. Measurement and modeling of gas transfer in cracked mortars. Mater Struct 2006;39(1):43–52.
[5] Reinhardt H-W, Jooss M. Permeability and self-healing of cracked concrete as function of temperature and crack width. Cem Concr Res 2003;33(7):981–5.
[6] Coussy O, Baroghel Bouny V, Dangla P, Mainguy M. Evaluation de la perméabilité à l'eau liquide des bétons à partir de leur perte de masse durant le séchage. In: Baroghel Bouny V, editor. Transferts dans les bétons et durabilité, Special Issue of Revue Française de Génie Civil, vol. 5(2–3). Paris: Hermès Science Publications; 2001.
[7] Rizkalla SH, Lau BL, Simmonds SH. Air leakage characteristics in reinforced concrete. J Struct Eng 1984;110(5):1142–69.
[8] Suzuki T, Takiguchi K, Ide Y, Kimura K. Leakage of gas through concrete walls, IABSE symposium. Paris; 1987.
[9] Ripphausen B. Untersuchungen zur Wasserdüchlässigkeit und sanierung von Stahlbetonbauteilen mit Trennrissen. PhD thesis. RWTH Aachen; 1989 [In German].
[10] Tsukamoto M. Untersuchung zu Durcklässigkeiten von faserfreien und faserverstärkten Betonbauteilen mit Trennrissen. DafStb, Heft 440; 1994 [In German].
[11] Clear CA. The effects of autogenous healing upon the leakage of water through cracks in concrete. Cement and concrete association, technical report n 559; 1985.
[12] Mivelaz P. Etanchéité des structures en béton armé, fuites au travers d'un élément fissuré. PhD thesis. EPFL; 1996 [In French].
[13] Buss W. Proof of leakage rate of a concrete reactor building. 3. ACI Special, Publication Sp-34; 1972. p. 1291–1320.
[14] MacGregor JG, Murray DW, Simmonds SH. Behaviour of prestressed concrete containment structures – a summary of findings, technical report. University of Alberta Department of civil engineering; 1980.
[15] Saito H, Inada Y, Shibata A, Yokosawa H, Leakage through cracks in RC shear walls (Dynamic behavior and functional integrity tests on RC shear walls), Smirt 11, vol.H, Tokyo; 1991.
[16] Baroghel Bouny V. Caractérisation des pâtes de ciment et des bétons-Méthodes, analyse, interprétations. PhD thesis. ENPC; 1994 [In French].
[17] Ranaivomanana H, Verdier J, Sellier A, Bourbon X. Toward a better comprehension and modeling of hysteresis cycles in the water sorption-desorption process for cement based materials. Cem Concr Res 2011;41(8):817–27.
[18] Gagné R, François R, Masse P. Chloride penetration testing of cracked mortar samples. In: Bahia N, Sakai K, Gjory OE, editors. Concrete under severe conditions 1, Vancouver; 2001. p 198–205.
[19] Bary B, Sellier A. Coupled moisture-carbon dioxide-calcium transfer model for carbonation of concrete. Cem Concr Res 2004;34(10):1859–72.
[20] Nishikawa T, Suzuki K, Ito S, Sato K, Takebe T. Decomposition of synthesized ettringite by carbonation. Cem Concr Res 1992;22(1):6–14.
[21] Adenot F. Durabilité du béton, caractérisation et modélisation des processus physiques et chimiques de dégradation du ciment. PhD thesis. Université d'Orléans; 1992.
[22] Papadakis VG, Vayenas CG, Fardis MN. Fundamental modelling and experimental investigation of concrete carbonation. ACI Mater J 1991;88(4):363–73.
[23] Schliessl P, Reuter C. Wasserdurchlässigkeit von Stahlbetonbauteilen im Zustand II (gerissene Betonzugzone). Institute of Building Materials Research: University of Technology, Aachen; 1992 [In German].